

Robust Nonlinear Control of Air-to-Fuel Ratio in Spark Ignition Engines

Paljoo Yoon

Mando Corporation

Seungbum Park, Wootaik Lee

Graduate Student from the Department of Automotive Engineering, Hanyang University

Myoungho Sunwoo*

Associate Professor from the Department of Automotive Engineering, Hanyang University

This paper presents a new approach to the AFR (Air-to-Fuel Ratio) control problem, which is based on the wide-band oxygen sensor output. The dedicated nonlinear controller is based on the feedback linearization technique. It is well known that the feedback linearizing control technique requires an exact model of the plant for the cancellation of plant nonlinearities. A sliding mode control scheme is applied which can effectively compensate the modeling uncertainties. The measurement time delay of an oxygen sensor limits the gain of the feedback controller. Hence, time delay compensation procedure is necessary for the improvement of control performance. The Smith predictor is adopted to compensate the effects of time delay. The simulation and experimental results show that the proposed controllers can effectively reduce the transient peaks of AFR in spite of fast tip-in and tip-out maneuvers of the throttle.

Key Words : Air-to-Fuel Ratio (AFR), Wide-Band Oxygen Sensor, Feedback Linearizing Control (FLC), Sliding Mode Control (SMC), Smith Predictor

1. Introduction

In recent years, researchers working in the engine control field have applied different control techniques to internal combustion engines (Guzzella, 1997; Park, 2000). Since the current engine control system shows poor transient control performance, the application of modern control techniques could provide significant benefits by improving the transient control performance of an engine. The linear control design approach based on the locally linearized model has been most popular for design of a closed-loop engine

controller. In order to apply linear control techniques, the dynamics of the plant must be reasonably linear. Unfortunately, while the mean value engine model characterizes engine dynamics well over the entire operating range of an engine (Yoon et al., 2000), the highly nonlinear nature of engine dynamics limits the use of linear controller design techniques. Therefore, it seems natural to develop a controller so that the nonlinear dynamics of an engine model can be used for the design of engine control systems.

The problem of the precise control of the AFR in SI engines is very crucial for the performance improvement of a three-way catalytic converter. However, the AFR control is a very difficult and challenging task because (Moraal, 1995)

- the air and fuel dynamics are highly nonlinear with a variable time delay.
- the fuel dynamics are dependent on engine operating conditions (such as temperature and engine speed) and may change over time.

* Corresponding Author,

E-mail : msunwoo@email.hanyang.ac.kr

TEL : +82-2-2290-0453; **FAX :** +82-2-2297-5495

Associate Professor from the Department of Automotive Engineering, Hanyang University 17 Haengdang-dong, Seongdong-gu, Seoul 133-791, Korea.(Manuscript Received September 9, 2000 ; Revised March 14, 2001)

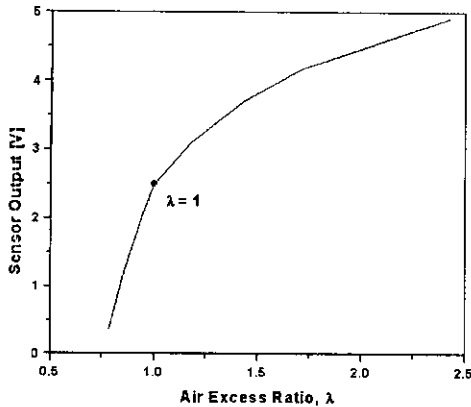


Fig. 1 Characteristics of wide-band oxygen sensor (Bosch LSU4)

• the only information available for feedback control is provided by a delayed measurement output from a binary oxygen sensor, a device which acts like a switch, indicating only whether the mixture is rich or lean, without indicating the degree of richness/leanness.

Conventional AFR controllers adopt a relatively simple linear PI (Proportional-Integral) controller via the feedback signal of a binary oxygen sensor. Due to the switching behavior of the oxygen sensor, limit cycles and relatively large excursions in AFR cannot be avoided. However, with the advent of wide-band oxygen sensors, nonlinear and more sophisticated control schemes will become viable. Figure 1 shows the characteristics of a wide-band oxygen sensor (or Universal Exhaust Gas Oxygen Sensor; UEGO Sensor) manufactured by Bosch. When the air excess ratio ($\lambda = \frac{\dot{m}_{ap}}{\beta_s \dot{m}_{fc}}$) is unity, the output voltage is 2.5 V. Unlike the binary oxygen sensor, the UEGO sensor can detect the quantitative AFR including the stoichiometric ratio. Therefore, the wide-band oxygen sensor makes it possible to employ advanced control schemes.

This paper presents a new approach to the AFR control problem, which is based on the wide-band oxygen sensor output. The dedicated nonlinear controller is based on the feedback linearization technique (Isidori, 1995). It is well known that the feedback linearizing control (FLC) technique requires an exact model of the

plant for the cancellation of plant nonlinearities. To overcome this problem, a sliding mode control (SMC) scheme, which can effectively compensate model uncertainties, is applied. Furthermore, the measurement time delay from an oxygen sensor limits the gain of the feedback controller. Hence, time delay compensation procedure is necessary for the control performance improvement. In this study, the Smith predictor is adopted to compensate for the effects of time delay.

2. Nonlinear AFR Controller Design Based on UEGO Sensor

2.1 Two-state engine model for AFR control

The two-state dynamic engine model, which was introduced in the previous study (Yoon, 2000) is used for designing a fuel injection controller.

With the conservation of mass in the intake manifold, the manifold pressure dynamic equation can be described as:

$$\dot{P}_m = \frac{RT_m}{V_m} (\dot{m}_{at} - \dot{m}_{ap}) \quad (1)$$

where \dot{m}_{at} is the mass airflow rate into the manifold, \dot{m}_{ap} is the mass airflow rate out of the manifold, R is the gas constant, T_m is the intake manifold air temperature, and V_m is the volume of intake manifold and surge tank. The mass air flow rate out of the manifold \dot{m}_{ap} can be obtained from a steady-state engine test using the speed-density algorithm as follows ;

$$\dot{m}_{ap} = \frac{V_D}{120RT_m} \eta_{vol} P_m N \quad (2)$$

Where V_D is the displacement volume of the engine, η_{vol} is the volumetric efficiency, and N is the engine speed. The quantity $\eta_{vol} \times P_m$ in Eq. (2) is called the normalized air charge, m_{an} (Hendricks et al., 1996; Yoon et al., 2000). The normalized air charge is obtained from the steady state engine test, and is approximated by a polynomial equation.

$$m_{an} = \eta_{vol} P_m = w_1(N) + w_2(N) P_m \quad (3)$$

where $w_1(N) = w_{10} + w_{11}N + w_{12}N^2 + w_{13}N^3 + w_{14}N^4$, $w_2(N) = w_{20} + w_{21}N + w_{22}N^2$

Using this relation, the mass air flow rate out of the manifold, \dot{m}_{ap} can be rewritten as

$$\begin{aligned}\dot{m}_{ap} &= \frac{V_D N \dot{m}_{an}}{120 R T_m} \\ &= \frac{V_D}{120 R T_m} N [w_1(N) + w_2(N) P_m] \quad (4)\end{aligned}$$

The mass air flow rate into the intake manifold, \dot{m}_{at} can be obtained as

$$\dot{m}_{at} = C_D \cdot MA \cdot TC(\alpha) \cdot PRI(P_m) \quad (5)$$

where C_D is the discharge coefficient of the throttle valve, MA is the maximum possible flow rate through the specific throttle valve, TC is a normalized flow as a function of the cross-sectional area, α is the throttle opening, and PRI is a normalized flow as a function of pressure ratio. Substituting Eqs. (4) and (5) into Eq. (1) yields

$$\begin{aligned}\frac{dP_m}{dt} &= \frac{V_D N}{120 V_m} [w_1(N) + w_2(N) P_m] \\ &\quad + \frac{R T_m}{V_m} \dot{m}_{at}(\alpha, P_m) \\ &= f(P_m, N) + d(\alpha, P_m) \quad (6)\end{aligned}$$

where

$$\begin{aligned}f(P_m, N) &= -\frac{V_D N}{120 V_m} [w_1(N) + w_2(N) P_m] \\ d(\alpha, P_m) &= \frac{R T_m}{V_m} \dot{m}_{at}(\alpha, P_m) \\ &= \frac{R T_m}{V_m} C_D \cdot MA \cdot TC \cdot PRI\end{aligned}$$

In this study, it will be assumed that the driver directly controls the throttle valve (i. e., the amount of air entering the intake manifold is a measurable disturbance but not controllable).

The characteristics of the fuel injection process is very complex and is largely influenced by various factors, such as injection schemes, spray patterns, injection timing, port geometry, intake manifold wall temperature, fuel rail pressure, and so on. However, it is actually somewhat difficult to implement such complicated fuel delivery models which consider all of the aspects mentioned above to real time engine control applications. Thus, the first order lumped parameter model is widely used to represent the fuel delivery process. A widely used model for the dynamics of fuel in an intake port is based on the

assumption that some fraction (X) of the injected fuel forms a film on the walls and the fuel in the film evaporates with time constant (Aquino, 1981).

$$\dot{m}_{ff} = -\frac{1}{\tau_f} m_{ff} + X \dot{m}_{fi} \quad (7)$$

$$\dot{m}_{fc} = (1-X) \dot{m}_{fi} + \frac{1}{\tau_f} m_{ff} \quad (8)$$

where m_{ff} is the mass of the fuel in the puddle, \dot{m}_{fi} is the injected fuel-mass-flow rate, \dot{m}_{fc} is the actual fuel-mass-flow rate into the cylinder, X is the fraction of injected fuel entering into the puddle, and τ_f is the evaporation time constant of the fuel puddle. From the cancellation of m_{ff} in Eqs. (7) and (8), the following fuel delivery model can be derived.

$$\dot{m}_{fc} = -\frac{1}{\tau_f} \dot{m}_{fc} + (1-X) \dot{m}_{fi} + \frac{1}{\tau_f} \dot{m}_{fi} \quad (9)$$

2.2 Feedback linearizing control (FLC)

The objective of the fuel injection control is to keep the AFR close to the stoichiometric ratio. It is equivalent to maintaining y at:

$$y = \frac{\dot{m}_{ap}}{\dot{m}_{fc}} = 14.7 \pm 0.2 = \beta_s \pm 0.2 \quad (10)$$

where β_s is a stoichiometric AFR. Differentiation of y with respect to time gives

$$\dot{y} = \frac{\dot{m}_{ap} \dot{m}_{fc} - \dot{m}_{fc} \dot{m}_{ap}}{m_{fc}^2} \quad (11)$$

In this equation, \dot{m}_{ap} can be obtained from the differentiation of Eq. (4).

$$\begin{aligned}\dot{m}_{ap} &= \frac{V_D}{120 R T_m} \left[\dot{N} w_1 + N \frac{\partial w_1}{\partial N} \dot{N} + \dot{N} w_2 P_m \right. \\ &\quad \left. + N \frac{\partial w_2}{\partial N} \dot{N} P_m + N w_2 \dot{P}_m \right] \quad (12)\end{aligned}$$

Since the crankshaft dynamics are much slower than those of the manifold pressure, $\dot{N} \approx 0$ is assumed to be zero. Therefore, \dot{m}_{ap} can be rewritten as

$$\begin{aligned}\dot{m}_{ap} &= \frac{V_D}{120 R T_m} N w_2(N) \dot{P}_m \\ &= \frac{V_D}{120 R T_m} N w_2(N) [f(P_m, N) \\ &\quad + d(\alpha, P_m)] \quad (13)\end{aligned}$$

Inserting Eqs. (9) and (13) into Eq. (11), the

following expression is obtained.

$$\begin{aligned} \dot{y} = & \frac{V_D}{120RT_m} \frac{Nw_2(N)}{m_{fc}} [f(P_m, N) + d(\alpha, P_m)] \\ & - \frac{V_D}{120RT_m} \frac{N}{m_{fc}^2} [w_1(N) + w_2(N)P_m] \\ & \cdot \left[\frac{\dot{m}_{fi} - \dot{m}_{fc}}{\tau_f} + (1-X)\dot{m}_{fi} \right] \end{aligned} \quad (14)$$

Equation (14) can be rewritten as

$$\dot{y} = \alpha(\alpha, P_m, N) + b(P_m, N)\dot{m}_{fi} \quad (15)$$

where

$$\begin{aligned} \alpha(\alpha, P_m, N) = & \frac{V_D}{120RT_m} \frac{Nw_2(N)}{m_{fc}} \\ & [f(P_m, N) + d(\alpha, P_m)] \\ & - \frac{V_D}{120RT_m} \frac{N}{m_{fc}^2} [w_1(N) + w_2(N)P_m] \\ & \cdot \left(\frac{\dot{m}_{fi} - \dot{m}_{fc}}{\tau_f} \right) \end{aligned} \quad (16)$$

$$b(P_m, N) = - \frac{V_D}{120RT_m} \frac{N}{m_{fc}^2} [w_1(N) + w_2(N)P_m] \cdot (1-X) \quad (17)$$

Since $b(P_m, N) \neq 0$ for all engine operating conditions, the control law

$$\dot{m}_{fi} = \frac{1}{b(P_m, N)} [-\alpha(\alpha, P_m, N) + v] \quad (18)$$

yields the linear system

$$\dot{y} = v \quad (19)$$

Letting $e = y - \beta_s$ be the error, and choosing the new input v as

$$v = \dot{\beta}_s - \kappa_1(y - \beta_s) \quad (20)$$

with κ_1 being a positive constant, the error dynamics of the closed-loop system is given by

$$\dot{e} + \kappa_1 e = 0 \quad (21)$$

which represents an exponentially stable dynamics. Furthermore, the linear controller in Eq. (20) must possess integral action for zero offset control in spite of constant disturbances.

$$v = \dot{\beta}_s - \kappa_1(y - \beta_s) - \kappa_2 \int_0^t (y - \beta_s) d\tau \quad (22)$$

The control law in Eq. (18) is in essence an output-zeroing controller that renders the unobservable part of the system's dynamics. This zero dynamics has to be proved to be inherently asymptotically stable (the system to be minimum phase) otherwise the proposed approach would

not be viable. It has been proven by the previous study (Guzzella, 1997) that the zero dynamics of the AFR control system is asymptotically stable under the assumption of constant disturbance.

2.3 Sliding mode control (SMC)

The feedback linearizing control law in the previous section requires exact knowledge of a plant model. In order to obtain a more globally robust control performance even under the modeling uncertainties, a sliding mode control approach is employed.

Define the sliding surface as

$$S = y - \beta_s \quad (23)$$

The differential equation for can be given by

$$\begin{aligned} \dot{S} = & \dot{y} - \dot{\beta}_s \\ = & \alpha(\alpha, P_m, N) + b(P_m, N)\dot{m}_{fi} - \xi \end{aligned} \quad (24)$$

where $\xi = \dot{\beta}_s = 0$.

In order to satisfy the sliding condition $S\dot{S} \leq -\kappa_d S^2 - \eta |S|$ (Zhang and Panda, 1999), the control input \dot{m}_{fi} can be chosen as

$$\begin{aligned} \dot{m}_{fi} = & \frac{1}{b(P_m, N)} \\ & [-\kappa_d S - \alpha(\alpha, P_m, N) + \xi - \eta \text{sgn}(S)] \end{aligned} \quad (25)$$

where κ_d is a strictly positive constant. Note that the sliding control law described in Eq. (25) is not smooth since the control law is discontinuous across the sliding surface so that undesirable chattering phenomenon occurs. This chattering can be smoothed out by using a saturation function (Slotine and Li, 1991) which replaces $\text{sgn}(S)$.

$$\begin{aligned} \dot{m}_{fi} = & \frac{1}{b(P_m, N)} \\ & \left[-\kappa_d S - \alpha(\alpha, P_m, N) + \xi - \eta \text{sat}\left(\frac{S}{\phi}\right) \right] \end{aligned} \quad (26)$$

where ϕ is called the thickness of the boundary layer and the saturation function is defined as

$$\text{sat}\left(\frac{S}{\phi}\right) \equiv \begin{cases} \frac{S}{\phi} & \text{if } |S| < \phi \\ \text{sgn}(S) & \text{if } |S| \geq \phi \end{cases} \quad (27)$$

3. Time Delay Compensation

The problem of constructing a control

algorithm that is capable of handling dead time is a key issue in many process control applications. When dead times are present in the control loop, the controller gains have to be reduced to maintain stability. A larger gain reduction is required for a larger dead time relative to the time scale of the process. Under most circumstances, this results in poor performance and sluggish responses. Powerful dead time compensation methods are available in literature for linear processes which are modeled with a rational transfer function with delay. The most popular technique is the well-known Smith predictor (Kravaris, 1989; Lewis, 1992).

The fuel injection control laws in the previous section are developed under the assumption of no measurement time delay in AFR. However, there is a considerable transport delay between fuel injection and the oxygen sensor measurement. The time delay is a function of engine operating conditions and can be identified by fuel perturbation tests. This time delay induces fuel injection control problems (Cho and Hedrick, 1988) such as

- increase in the chatter magnitude of AFR
- decrease in chatter frequency
- decrease in the attractiveness of AFR toward stoichiometry by the amounts proportional to the amount of time delay

This section will briefly review the time delay compensation technique, and apply the results to the AFR control problem in SI engines.

3.1 Classical Smith predictor

The principle behind the time delay compensating controller is the prediction of the future changes in the measurement signal. This can be achieved by feeding the control signal through a model of the process. One approach to compensate time delay is the Smith predictor. The structure of the smith predictor is in Fig. 2.

Assume that the plant is asymptotically stable, and that it can be described by a rational transfer function plus delay, i.e. $G_p(s)e^{-Ts}$. A simple analysis of Fig. 2 is that if $G_p(s)=G_m(s)$ and $T=T_m$, then a controller transfer function $G_c(s)$ can be synthesized as a standard feedback

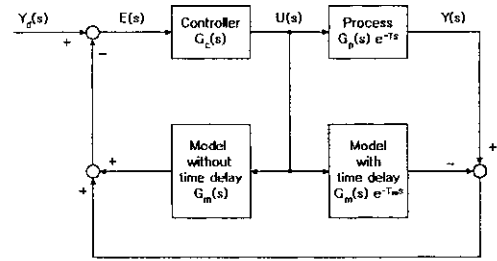


Fig. 2 The structure of Smith predictor

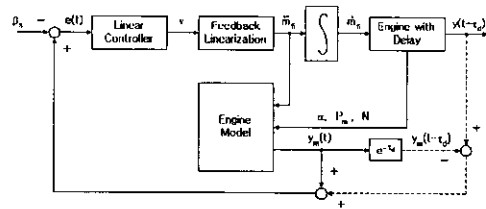


Fig. 3 Fuel injection control law with Smith predictor

regulator for a delay-free process described by $G_p(s)$. This means that we can design a controller to improve the closed-loop system performance as if the process is without time delay.

Time delay, dead time or time lag, when it occurs, causes a phase lag in the system. Therefore, a phase lead is needed to compensate a phase lag. The Smith predictor has been known to provide a significant phase lead.

3.2 Nonlinear extension of the Smith predictor for AFR control

Kravaris and Wright (1989) have developed a nonlinear extension of the Smith predictor based on the feedback linearization theory. Their feedback linearizing control structure can easily be applied to the AFR control problem as depicted in Fig. 3 where $y_m(t)$ is the delay-free output of the model, $y_m(t - \tau_d)$ is the delayed model output, and $y(t - \tau_d)$ is the delayed output of an actual engine.

Ignoring the dashed lines, a delay-free model of the plant is used to generate the output signal. To help account for errors in the delay-free model, the delay itself is also modeled and used to generate a delayed model output. The dashed lines show how the delayed model output is

compared with the actual output so that a modeling error is fed back into the control loop. In this way, the effect of errors in the model is reduced. The predicted output signal for the error calculation is given by

$$\hat{y}(t) = y_m(t) + y(t - \tau_d) - y_m(t - \tau_d), \quad (28)$$

and the error signal is defined as

$$e(t) = \hat{y}(t) - \beta_s. \quad (29)$$

If the engine model in Fig. 3 is exactly identical to the actual engine dynamics, the fuel injection control law in Eq. (18) or (26) can easily be implemented as if there is no measurement delay. However, the performance of the controller with the Smith predictor largely depends on the accuracy of the plant model (particularly, the accuracy of the time delay).

4. Simulation Results

In order to validate the effectiveness of the proposed fuel injection control law, simulation studies are conducted. The engine model used in the simulation is comprised of three input variables (throttle angle, fuel flow rate, and spark timing) and one disturbance (load torque). The model is described with three state variables (intake manifold pressure, engine speed, and fuel mass in the fuel film), and major subsystems (mass airflow through throttle, torque production model, etc.) of the engine expressed in algebraic equations are included. The detailed expressions of each subsystem are explained in (Kravaris, 1989).

For the performance evaluation of the proposed controller, the throttle angle is changed as shown in Fig. 4, to simulate a fast tip-in and tip-out situation which allows the engine to be operated between 1500 and 3500 rpm (See Fig. 5). The sampling interval for the simulation is selected to synchronize with the intake event of an engine because of the event-based nature of the engine. UEGO sensor is assumed to have measurement delay of three engine cycle.

First, the performance of a linear PI controller is demonstrated with and without the Smith

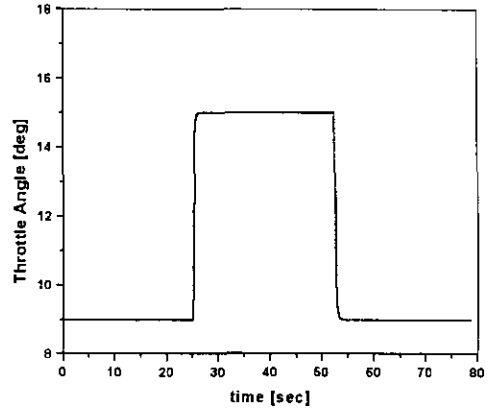


Fig. 4 Throttle angle pattern: simulation

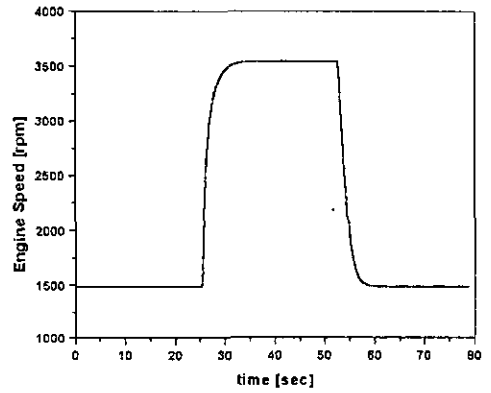


Fig. 5 Engine speed: simulation

predictor. A perfect engine model is assumed in this simulation. The fuel injection time t_{inj} is given as follows;

$$t_{inj} = (t_{inj})_{base} \left[1 + K_p \left(e(t) + \frac{1}{T_i} \int_0^t e(\tau) d\tau \right) \right] \quad (30)$$

In Eq. (30), the steady state fuel injection time $(t_{inj})_{base}$ can be calculated from the following relations.

$$(\dot{m}_{fi})_{base} = \frac{\dot{m}_{ap}}{\lambda_s \beta_s} = \frac{V_D m_{an} N}{120 R T_m \lambda_s \beta_s}, \quad (31)$$

$$(m_{fi})_{base} = \frac{30 (\dot{m}_{fi})_{base}}{N}, \quad (32)$$

$$(t_{inj})_{base} = \frac{(m_{fi})_{base}}{K_{inj}} + t_o \quad (33)$$

where K_{inj} and t_o are the coefficients of the injector characteristics. Figure. 6 shows the simulation results of the linear PI controller of

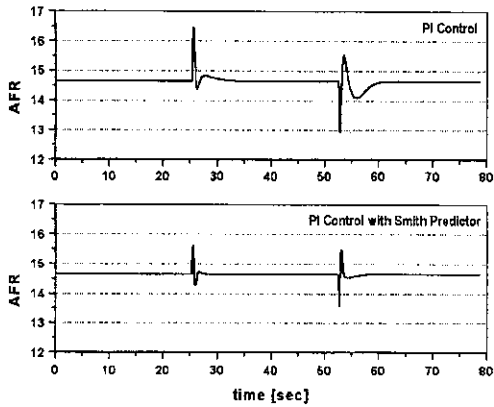


Fig. 6 Performance of linear PI Controller with and without Smith predictor: simulation

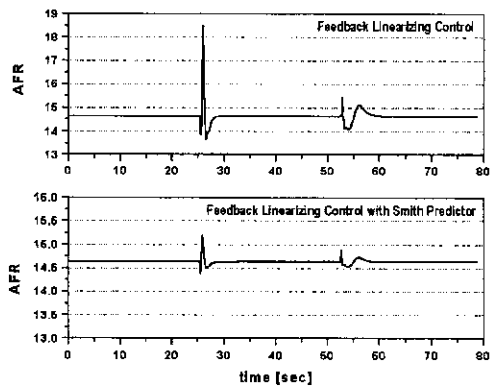


Fig. 7 Performance of FLC with and without Smith predictor: simulation

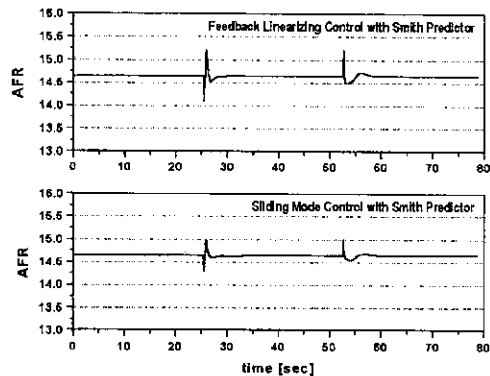


Fig. 8 Performance of FLC and SMC with modeling error: simulation

are chosen to be ten times larger than those of the linear PI controller without the predictor. The linear PI controller without the Smith predictor shows unstable control performance with about ten times larger gain. The poles of linear PI controller are $-0.78 \pm 9.03i$ and -0.98 , and the poles of linear PI controller with Smith predictor are -132.06 and -0.85 at fixed operating point (1500rpm and 0.6bar). As shown in this figure, the transient peaks in the lower graph are relatively smaller than those of the upper graph. However, the AFR response is still unsatisfactory because the linear controller provides no mechanism for coping with the nonlinearities of the engine.

Second, the performance of the feedback linearizing control law in Eq. (18) is demonstrated for the case with and without the prediction mechanism. The gains of the linear controller in Eq. (22) with the predictor are selected to be four times larger than those of the controller without the predictor. The upper graph in Fig. 7 represents the performance of FLC with no prediction mechanism. Due to a measurement delay from an UEGO sensor, the gains of the controller are limited to a relatively smaller value than those of FLC with the predictor. Therefore, large transient peaks from a fast tip-in/tip-out maneuver of a throttle are unavoidable. However, by applying the Smith predictor to the control law, the gains of the controller can be increased without instability problem. As shown in the lower graph of Fig. 7, the transient peaks in AFR are substantially reduced, and the results are very close to the control objective as described in Eq. (10).

To investigate the effect of model error on control performance, 20% additive uncertainties in the parameters of the fuel delivery model (i. e. X and τ_f) is assumed. As shown in the upper graph of Fig. 8, the control performance of a feedback linearizing AFR controller is slightly degraded due to model error in the fuel delivery model. It is well known that the sliding mode control can directly consider robustness under model uncertainties and disturbances in the design process. The lower graph of Fig. 8 re-

Eq. (30). The proportional and integral gains of the linear PI controller with the Smith predictor

presents the simulation results of the sliding mode fuel injection control law in Eq. (26) with the Smith predictor. The sliding mode controller shows a similar control performance to the feedback linearizing controller with the exact model.

The sliding mode control law shows the best performance in spite of model uncertainties. The allowable error in time delay is about five engine stroke with the gain used in simulation, and that is large enough to be implemented in practice.

The last simulation indicates that the model uncertainties can be overcome by use of robust control schemes. However, the dead time should be known exactly since the uncertainties in time delay have the most critical effect on the performance of the closed-loop system.

5. Experimental Results

For the performance evaluation of the proposed control schemes, a 2.0L, inline 4 cylinder DOHC engine and eddy current type dynamometer are used. The ignition timing, fuel injection timing and duration are controlled by a PC-based engine control system (ECS) developed at Hanyang University (Yoon et al., 1998). The ignition and fuel injection of each cylinder can be precisely controlled by the ECS with the use of a crankshaft encoder and a cam sensor. Therefore, the ECS is operated not in time-base but in event-base. This means that the ignition and fuel injection can be updated at each event of every engine cycle (i.e. crank angle 180° at 4 cylinder, 4 stroke engine). An eight channel analog-to-digital converter, which the ECS employs, is used for the purpose of data acquisition and closed-loop control. The analog signals from the engine-dynamometer system, such as intake manifold pressure, mass airflow rate into manifold, AFR, and throttle angle are measured at each engine event. A wide-band oxygen sensor (Bosch LSU4) is used for closed-loop control purpose. The control algorithm is implemented using a Pentium PC, and the control loop is executed with each engine event.

Figure 9 shows the throttle pattern for the performance evaluation of the three kinds of AFR

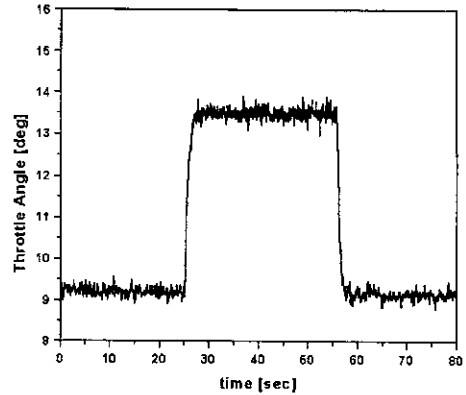


Fig. 9 Throttle angle pattern: experiment

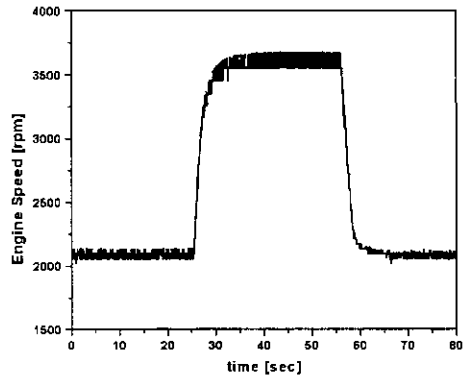


Fig. 10 Engine speed: experiment

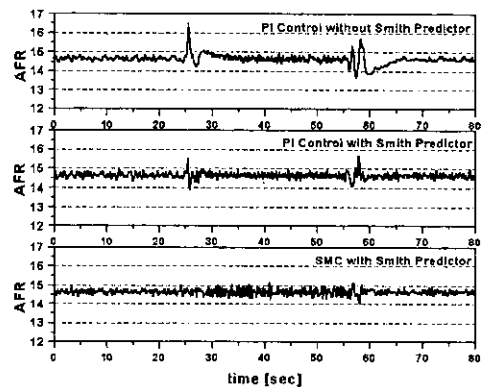


Fig. 11 Performance evaluation of various types of AFR controllers: experiment

controllers such as the linear PI controller with and without prediction mechanism and the SMC with the Smith predictor. Figure 10 represents the corresponding engine speed under the condition of a fixed load of dynamometer. Figure 11 shows

the experimental results with the three kinds of AFR controller. The upper graph shows the AFR response of the conventional linear PI controller.

The AFR response similar to the simulation results represented in the upper graph of Fig. 6, shows relatively large transient peaks and sluggish response after the transients. The center graph represents the AFR response in the case of the linear PI controller with Smith predictor. Due to the prediction mechanism presented in the control loop, the experimental results show the improved disturbance rejection performance in comparison with the linear PI controller without the Smith predictor. However, this kind of the linear control structure cannot effectively compensate for the engine nonlinearities, and the control performance is far from the control objective represented in Eq. (10). The lower graph shows the result of the AFR of the proposed sliding mode fuel injection controller with the Smith predictor. It can be seen that the AFR has no large transient peaks, and the SMC with the Smith predictor meets the control objective described in Eq. (10).

6. Conclusions

The AFR control algorithm developed in this paper employs a sliding mode fuel injection control law with a Smith predictor based on the measurement of a wide-band oxygen sensor. The dedicated nonlinear controller is based on the feedback linearization technique. It is well known that the feedback linearizing control technique requires an exact model of the plant for the cancellation of plant nonlinearities. To overcome this problem, a sliding mode controller is applied which can effectively treat the modeling uncertainties. Furthermore, the measurement time delay in the oxygen sensor limits the gain of feedback controller. Hence, time delay compensation procedure is necessary for the improvement of the performance of the controller. The Smith predictor is adopted in this study to compensate for the effects of time delay. The simulation and experimental results show that the proposed controller can effectively reduce the transient peaks of

AFR in spite of fast tip-in and tip-out maneuvers of the throttle.

References

- Aquino, C. F., 1981, "Transient A/F Control Characteristics of the 5 Liter Central Fuel Injection Engine," *SAE Paper* No. 810494.
- Cho, D. and Hedrick, J. K., 1988, "A Nonlinear Controller Design Method for Fuel-Injected Automotive Engines," *Transactions of ASME, Journal of Engineering for Gas Turbines and Power*, Vol. 110, No. 3, pp. 313~320.
- Guzzella, L., Simons, M. and Geering, H. P., 1997, "Feedback Linearizing Air/Fuel Ratio Controller," *Control Engineering Practice*, Vol. 5, No. 8, pp. 1101~1105.
- Hendricks, E., Chevalier, A., Jensen, A. and Sorenson, S. C., 1996, "Modeling of Intake Manifold Filling Dynamics," *SAE Paper* No. 960037.
- Isidori, A., 1995, *Nonlinear Control Systems*, Springer, pp. 137~218.
- Kravaris, C. and Wright, R. A., 1989, "Dead Time Compensation for Nonlinear Processes," *AIChE Journal*, Vol. 35, No. 9, pp. 1535~1542.
- Lewis, F. L., 1992, *Applied Optimal Control and Estimation*, Prentice-Hall, pp. 270~278.
- Moraal, P. E., 1995, "Adaptive Compensation of Fuel Dynamics in SI Engine Using a Switching EGO Sensor," *Proceedings of the 34th IEEE Conference on Decision and Control*, pp. 661~666.
- Park, S., Yoon, P. and Sunwoo, M., 2000, "SI Engine Closed-loop Spark Advance Control Using Cylinder Pressure," *Transactions of KSME Part A*, Vol. 24, No. 9, pp. 2361~2370 (in Korean)
- Slotine, J.-J. E. and Li, W., 1991, *Applied Nonlinear Control*, Prentice-Hall, Englewood Cliffs, pp. 276~310.
- Yoon, P., Kim, M. and Sunwoo, M., 1998, "A Study on Design and Development of an Engine Control System based on Crank Angle," *Transactions of KSAE*, Vol. 6, No. 4, pp. 198~210 (in Korean).
- Yoon, P., Park, S. and Sunwoo, M., 2000, "A Nonlinear Dynamic Model of SI Engines for

Designing Controller," *FISITA world automotive congress*, F2000A177.

Zhang, D. Q. and Panda, S. K., 1999,

"Chattering-Free and Fast Response Sliding Mode Controller," *IEE Proc. -Control Theory Appl.*, Vol. 146, No. 2, pp. 171~177.